SPE Asia Pacific Oil & Gas Conference and Exhibition
2016

SPE-182291-MS

Old Technique New Insights: Reservoir Properties from Pulse Testing

Bert Filippi and Amin Nabipour, OPES International Pty Ltd,
Naoki Fukuda, Tokyo Gas Co. Ltd.

Abstract

Pulse testing, introduced in the 1960's, is a useful analytical technique to detect communication between wells and estimate interconnected reservoir properties. Despite its potential, it is rarely included in data acquisition programs. This is probably because engineers prefer to use interference testing, which can be easily detected and interpreted by reservoir simulation. Regretfully, the latter cannot analyse pulses which are so subtle that they are hidden within the tidal effects of pressure measurement.

In pulse testing, interconnected permeability is calculated from the time the pulse takes to travel from the producer to the observation well. In this paper, new formulations are presented for both linear and radial flow regimes. These are straightforward, making their application easy. Furthermore, they can detect whether pressure is propagated along channels or more extensive areal systems. The magnitude of the pulse can also provide invaluable reservoir characterisation. For a relatively homogenous system, this amplitude is easily calculated using either radial or linear coordinates. For more complex geometries, such as communication between different sands, detailed studies are required to quantify where and how the connectivity occurs between the producer and the observation well.

Often the pulse is significantly less than 0.1 psi which makes detection difficult, because of tidal effects, and analysis hard to interpret by finite difference simulation. Searching for such subtle changes in pressure takes perseverance. Calculating interconnected permeability by a single equation and determining the geometry of a channel by simple algebra makes the effort rewarding.

Three examples are presented to show how the following equations can be used to determine interconnected reservoir characteristics. Although the data is real, it refers to different fields, the interpretation of which is yet to be finalised. For this reason they are referred to as hypothetical cases A, B and C. These were selected because of the high frequency and the excellent quality of the data.

For linear flow $k = 79 \cdot x^2 \phi\mu c \cdot (\frac{1}{t_l} - \frac{1}{t}) / \ln \frac{t}{t_l}$

For radial flow $k = \frac{79 \cdot r^2 \phi\mu c}{2} (\frac{1}{t_l} - \frac{1}{t}) / \ln \frac{t}{t_l}$

In oil field units: k, x, r, ϕ, μ, c are permeability, distances (x and r), porosity, viscosity and compressibility. The times, t and t_l are the hours from the beginning and the end of production pulse (of duration t-t_l) to the maximum pressure disturbance at the observation well.

Introduction

Pulse testing was introduced by Johnson et al. (1966) as a useful technique to describe formation properties between wells. A sensitive gauge is used to monitor pressure in an observation well to detect the effect of short production pulses generated from an adjacent producer. Such information is invaluable, particularly at the early life of a field, where limited subsurface data are available. McKinley et al. (1968) reported the successful application of the technique in several well pairs and noted a number of advantages of pulse testing over other well testing methods. Rathbone et al. (1981) later used the technique for Statfjord oil field to determine the inter-layer communication. This was necessary for reservoir modelling and prediction of gas breakthrough into the wells. Brigham (1970) presented correlation charts to estimate reservoir properties, including transmissibility and storativity, from the time lag and pressure response amplitude in a pulse test.

Braisted et al. (1993), by pulse test analysis in the Fortescue development, identified the existence of a more complex geometry at the eastern side of the field. All the tests pointed to multidarcy permeability within and between reservoir units. Subsequent seismic data supported these findings.

Pulse testing pressure data normally contains different noises, which may impede the application of the technique. To tackle this issue, Toth and Megyery (1997) developed a cycle-sum-up method of evaluation and noise suppression. El-Khatib (2011) pointed out that the use of maximum pressure change to estimate reservoir properties introduces an error due to the production history of the observation well. He presented methods to correct the past pressure trend of the observation well in analysis of single (El-Khatib, 2011) and multiple pulse tests (El-Khatib, 2013).

Most work published on the pulse testing subject consider radial flow configuration. Many reservoirs, however, exhibit linear flow characteristics. This flow regime can be dominant due to structural reasons. An example is a reservoir containing multiple parallel faults which act as flow barriers. Certain depositional environments can also lead to a linear flow regime. One of the most well-known such scenarios is channel sand reservoirs.

In this study the analytical formulae applicable to pulse testing are derived for both linear and radial flow regimes. The equations are simple and can be easily used to estimate average permeability between the producer and observation well. One can then use this estimated permeability in the pulse testing equations to obtain information regarding reservoir geometry.

Theory

This section covers the mathematics for deriving simple formulae for pulse testing. Firstly, the linear flow solution is discussed followed by the radial flow regime. Finally, limitations of finite difference equation, for pulse testing applications, are also discussed.

Linear Flow Solution

Ehlig-Economides and Economids (1985) investigated the pressure transients in elongated linear flow systems. They used the work carried out by Miller (1962) on water influx and expanded it for interference analysis applications. In a linear flow configuration, the well is located in a rectangular channel of infinite length. The production and observation wells are separated by a distance sufficient for flow to be linear. This is visualised in the following diagram. Parameters shown are the distance between the wells (x), width (b) and height (h).

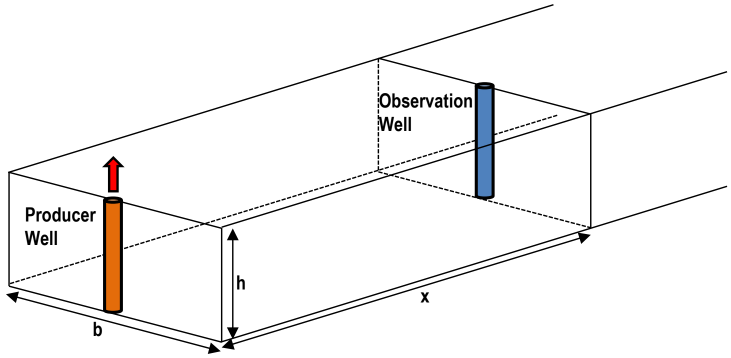

Figure 1 Schematic of linear flow configuration

Ehlig-Economides and Economids (1985) present the following equation for pressure disturbance due to production rate *q*, as a function of time and distance:

$$p(x,t) = p_i - \frac{(q/2)\mu}{khb}\left[2\sqrt{\frac{\eta t}{\pi}}\exp\left(\frac{-x^2}{4\eta t}\right) - (x)erfc\left(\frac{x}{2\sqrt{\eta t}}\right)\right] \quad \textbf{Equation 1}$$

where $\eta = \dfrac{k}{\varphi\mu c}$ is the formation diffusivity. The 0.5 multiple used for the flow rate is to take into account the flow from both sides of the production well. The above formula is in Darcy units, which are listed below, together with oil field units.

Table 1 Parameters in Darcy and Oil Field units

Parameter	Description	Darcy Units	Oil Field Units
φ	Porosity	fraction	fraction
μ	Viscosity	cP	cP
c	Compressibility	atm^{-1}	psi^{-1}
x	Distance between wells	cm	ft
t	Time	seconds	hours
k	Permeability	Darcy	mD
b	Width	cm	ft
p	Pressure	atm	psi
p_i	Initial pressure	atm	psi
q	Reservoir Flow rate	cc^3/sec	bbl/day

In the above formula the well is approximated as a planar source, which is consistent with the linear flow assumption. Its derivation also involves other inherent assumptions, such as homogeneity, isotropy, horizontal monophasic and laminar flow with constant viscosity and compressibility. Equation 1 can be re-written using the error function (erf) as below:

$$p(x,t) = p_i - \frac{(q/2)\mu}{khb}\left[2\sqrt{\frac{\eta t}{\pi}}\exp\left(\frac{-x^2}{4\eta t}\right) - x + (x)erf\left(\frac{x}{2\sqrt{\eta t}}\right)\right] \quad \textbf{Equation 2}$$

Given the definition of error function:

$$erf(\zeta) = \frac{2}{\sqrt{\pi}}\int_0^{\zeta} e^{-t^2}\,dt$$

the derivative of this function is obtained as follows:

$$\frac{derf(\zeta)}{d\zeta}=\frac{2e^{-\zeta^2}}{\sqrt{\pi}}$$

By defining $\zeta=\frac{x}{2\sqrt{\eta t}}$ and $Q=\frac{(q/2)\mu}{khb}$, Equation 2 can be differentiated with respect to time (t) as shown below:

$$\frac{dp(x,t)}{dt}=Q\left[\frac{2}{2}\sqrt{\frac{\eta}{\pi t}}\exp\left(\frac{-x^2}{4\eta t}\right)+\frac{x^2}{2t}\sqrt{\frac{1}{\pi\eta t}}\exp\left(\frac{-x^2}{4\eta t}\right)-\frac{x^2}{2t}\sqrt{\frac{1}{\pi\eta t}}\exp\left(\frac{-x^2}{4\eta t}\right)\right]$$

$$\frac{dp(x,t)}{dt}=Q\left[\sqrt{\frac{\eta}{\pi t}}\exp\left(\frac{-x^2}{4\eta t}\right)\right] \quad \text{Equation 3}$$

This is a surprisingly simple equation.

In a single pulse test the production well is opened, for a relatively short period, to generate a pressure pulse. Given there is connectivity, this will result in a pressure disturbance in an observation well located at distance x from the producer. Figure 2 is a schematic of the rate pulse at the producer and the pressure measured at the observation well. The latter reaches a minimum response when the first pressure derivative is zero. The time lag from end of pulse to this minimum point is denoted as t_l and the duration of the pulse is t_o.

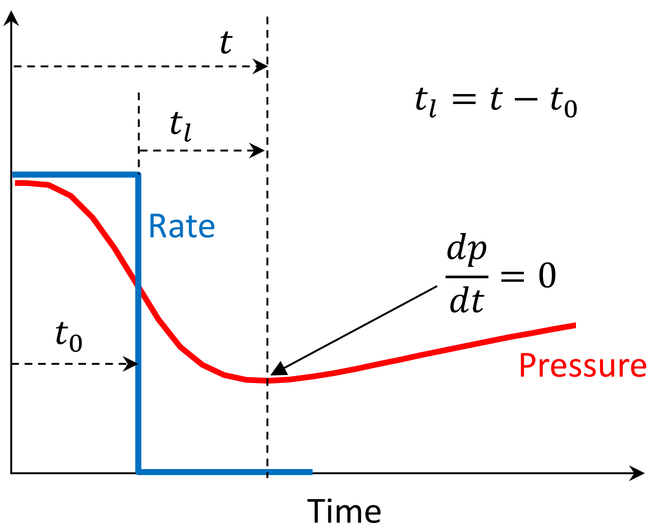

Figure 2 Schematic of rate and pressure in a pulse test

Using the superposition principle, the pulse can be considered to be generated by the combined effect of production at rate q for a period of t and at rate $-q$ for a period of t_l. Applying these conditions, Equation 3 generates the following:

$$\frac{dp}{dt}=0=Q\left[\exp\left(\frac{-x^2}{4\eta t}\right)\sqrt{\frac{\eta}{\pi t}}-\exp\left(\frac{-x^2}{4\eta t_l}\right)\sqrt{\frac{\eta}{\pi t_l}}\right]$$

$$\left[\exp\left(\frac{-x^2}{4\eta t}-\frac{x^2}{4\eta t_l}\right)\right]=\left(\frac{t}{t_l}\right)^{1/2}$$

$$\frac{x^2}{4\eta}\left(\frac{1}{t_l}-\frac{1}{t}\right)=\frac{1}{2}\ln\left(\frac{t}{t_l}\right)$$

Solving for k, this results in:

$$k=\frac{\phi\mu c x^2}{2}\left(\frac{1}{t_l}-\frac{1}{t}\right)/\ln\left(\frac{t}{t_l}\right)$$ which, in oil field units, takes the following form:

$$k=79\cdot x^2\phi\mu c\cdot(\frac{1}{t_l}-\frac{1}{t})/\ln\frac{t}{t_l}$$ .... **Equation 4**

The above simple equation estimates average permeability between producer and observation wells in a reservoir with prevailing linear flow regime. It is important to note that the above formula is independent of rate (q) and geometry (h and b) of the channel. It only requires values of time (t & t_l) and interconnected x and $\phi\mu c$.

In order to define the shape and amplitude of the pulse, however, the entire pressure time function is required. This can be derived from Equation 2 and is shown below. Although complex, it is easily computed in a spreadsheet application in a matter of minutes.

$$p(x,t)=p_i-\frac{(q/2)\mu}{khb}\left[2\sqrt{\frac{\eta t}{\pi}}\exp\left(\frac{-x^2}{4\eta t}\right)-x+(x)erf\left(\frac{x}{2\sqrt{\eta t}}\right)-2\sqrt{\frac{\eta t_l}{\pi}}\exp\left(\frac{-x^2}{4\eta t_l}\right)+x-(x)erf\left(\frac{x}{2\sqrt{\eta t_l}}\right)\right]$$ ... **Equation 5**

Radial Flow Solution

In this section the mathematics are shown for pulse testing in a radial flow regime configuration. Figure 3 shows a schematic of such a reservoir in which the observation well is located at a distance r from the producer well. The wells are confined in a wedge shape drainage area with an angle α. For a completely open reservoir, the angle α is 360^{o} and the shape becomes a cylinder.

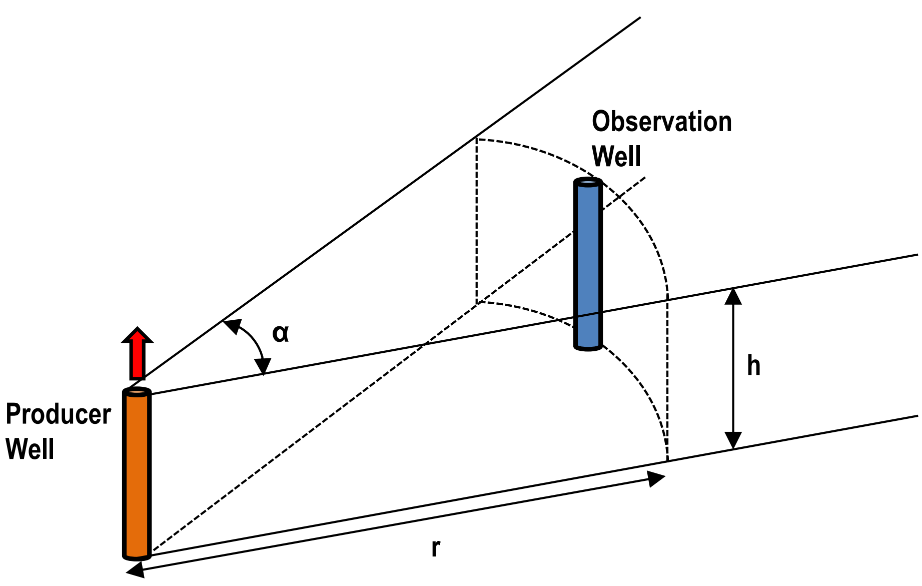

Figure 3 Schematic of radial flow configuration

For a production pulse q of duration t_0 as per Figure 2, the pressure response at distance r and time t (where $t > t_0$ and $t_l = t - t_0$) the equation below describes the build-up emulated by superimposing a negative flow rate of $-q$ after t_0.

$$p(r,t) = p_i - \frac{q\mu B}{4\pi kh\frac{\alpha}{360}}\left[Ei(-\frac{\phi\mu cr^2}{4kt}) - Ei(-\frac{\phi\mu cr^2}{4kt_l})\right] \qquad \textbf{Equation 6}$$

where the exponential integral (Ei) function is defined as $Ei(t) = \int_t^{\infty}\frac{e^{-\lambda}}{\lambda}d\lambda$ and $\lambda = \frac{\phi\mu cr^2}{4kt}$. All the parameters are in Darcy units. Note, for a cylinder shape area, the term $\frac{\alpha}{360}$ becomes 1.

Considering that $d\lambda / dt = -\frac{\lambda}{t}$, the differentiation of Equation 6 becomes almost trivial. By differentiating *p(r,t)*, with respect to time and equating it to zero, the following equation is obtained:

$$\frac{dp}{dt} = \frac{e^{-\lambda t}}{\lambda_t}(-\frac{\lambda_t}{t}) + \frac{e^{-\lambda tl}}{\lambda_{tl}}(\frac{\lambda_{tl}}{t_l}) = 0$$

Recalling that the hydraulic diffusivity is $\eta = \frac{k}{\phi\mu c}$ the above simplifies further:

$$-\exp(-\frac{r^2}{4\eta t})(\frac{1}{t}) + \exp(-\frac{r^2}{4\eta t_l})(\frac{1}{t_l}) = 0$$

$$-\exp(-\frac{r^2}{4\eta t} + \frac{r^2}{4\eta t_l}) = \frac{t}{t_l}$$

Rearranging the above and solving for k results in

$$k = \frac{r^2\phi\mu c}{4}(\frac{1}{t_l} - \frac{1}{t}) / \ln\frac{t}{t_l}$$

Although the formulation is slightly different, it is equivalent to the famous equation presented by Johnson et al. (1966). In oil field units, the above formula takes the following form:

$$k = \frac{79 \cdot r^2\phi\mu c}{2}(\frac{1}{t_l} - \frac{1}{t}) / \ln\frac{t}{t_l} \qquad \textbf{Equation 7}$$

The above formulation (radial) only differs from Equation 4 (linear) by a factor of 2. There are significant differences, however, between Equations 6 [$p(r,t)$] and 5 [$p(x,t)$] as shown in the plot below. The pressure difference, shown in the plot, is defined as $p(r,t) - p_i$.

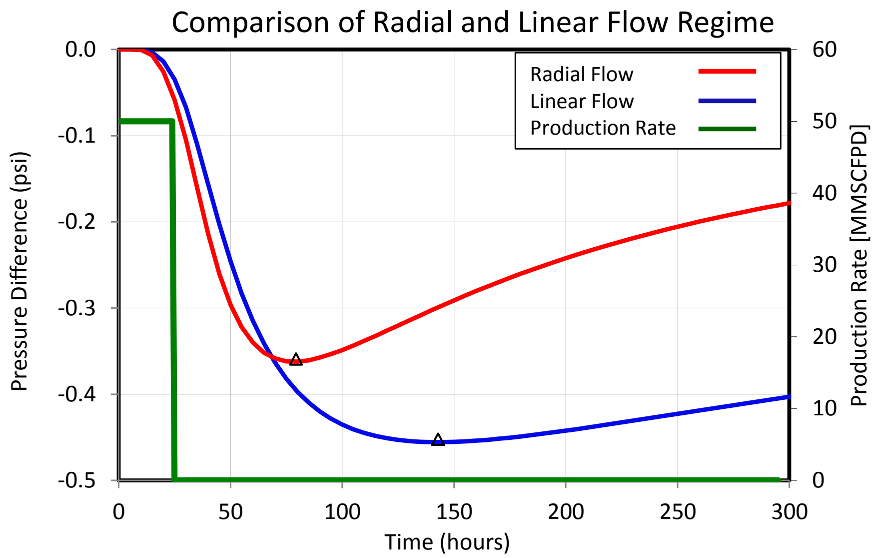

Figure 4 Comparison Pulse Test in Linear and Radial Flow Configurations

The following table summarises the parameters used in the calculations. As can be seen, both equations use the same parameters except for *b* and *α* which are specific to linear and flow regimes, respectively.

Table 2 Summary of parameters used for linear and flow configurations

Parameter (unit)	Value
p_i (psi)	3,000
φ (fraction)	.15
μ (cP)	.019
c (psi^{-1})	3×10^{-4}
x or r (ft)	8,000
h (ft)	400
k (mD)	800
b (ft) for linear flow	1,100
α (°) for radial flow	30
t_o (hrs)	24
q (MMscf/d)	50
q (equivalent bbl/d)	55,000

The plots show, in both flow regimes, the pressure difference in the observation well reaches a maximum (hence, a minimum absolute pressure) due to a production pulse in the producer. These pressure minima are denoted by black triangles in the figure. It is evident that the maximum response occurs sooner in the radial regime. In this particular case, the amplitude of the response is greater in the reservoir which is contained within a channel. With a large *α* angle for the radial case, the difference in amplitude between two regimes would be even more. Of importance is also the dissimilarity of pressure build-up trends between two flows. These opposing characteristics are clear indicators of the prevailing flow regime.

Finite Difference Approximation and Pulse Testing

Reservoir simulation is the ubiquitous tool in all aspects of reservoir analysis. Its limitations, however, are often ignored or not clearly understood. Pulse testing is such a case. In finite difference, the derivatives are generally approximated by the first term of the Taylor series which, irrespective of the formulation[1] in its simplest form, is exemplified as follows

$$\frac{dF(x)}{dx} = F'(x) \approx \frac{(F(x+\Delta x) - F(x))}{\Delta x} \quad \text{.......... Equation 8}$$

This is a poor approximation of the actual function shown below where the error is shown in square parenthesis.

$$F(x+\Delta x) = F(x) + \Delta x F'(x) + \frac{\Delta x^2 F''(x)}{(2!)} + \frac{\Delta x^3 F'''(x)}{(3!)} + \dots\dots$$

$$\frac{dF(x)}{dx} = \frac{(F(x+\Delta x) - F(x))}{\Delta x} + \left[\frac{\Delta x^2 F''(x)}{(2!)} + \frac{\Delta x^3 F'''(x)}{(3!)} + \dots\right]$$

For the case of the second differential, $F''(x)$, the error can be more severe. In contrast, when calculating the $Ei(\lambda)$ function for the radial flow such an approximation would not capture subtle pulses. This matter is visualised in the formulation shown below:

$$Ei(\lambda) = \int_t^\infty \frac{e^{-\lambda}}{\lambda} d\lambda = 0.5772 + Ln(\lambda) + \lambda^2/(2\cdot 2!) + \lambda^3/(3\cdot 3!) + \dots + \lambda^n/(n\cdot n!) + \dots$$

which required up to 10 terms to generate the response shown in the plot above. This was also the case for the linear flow regime, shown by the formulation below

$$erf(\lambda) = \frac{2}{\sqrt{\pi}} \int_t^\infty e^{-t^2} dt = \frac{2}{\sqrt{\pi}} (\lambda - \frac{\lambda^3}{3} + \frac{\lambda^5}{5\cdot 2!} - \frac{\lambda 7}{7\cdot 3!} \dots\dots + \frac{\lambda 47}{47\cdot 24!} - \dots)$$

Because of the oscillations in the finite difference simulation, subtle pulses cannot be emulated by this technique, no matter how fine the grid. It is for this reason that an analytical solution should be the first step in the analysis of pulse or, for that matter, interference testing. Once the pulse has been identified and interconnected properties defined, it is possible to utilise a simulator to investigate the effect of complex geometry by matching the diminution of the pulse amplitude. This may necessitate simulating a much greater pulse and investigating the geometry which attenuates the size of the observed pulse.

Application on Field Data

This section contains three examples of field application of the formulae discussed above.

Case A

The first case study is a reservoir where both the producer and the observation wells are completed in the same sand body, and interpreted as extensive, contiguous and relatively homogeneous. Geological mappings suggest the radial flow to be the dominant regime. The following plot shows the pressure at the observation well after the producer generated a 32-hour deep pulse. The proximity of the two wells and continuity of the sands generated almost a 1 psi amplitude pulse, which is clearly detectable and easily interpreted. The raw data is shown by the red line which exhibits the oscillation of tidal effects.

[1] Forward, backward or central difference

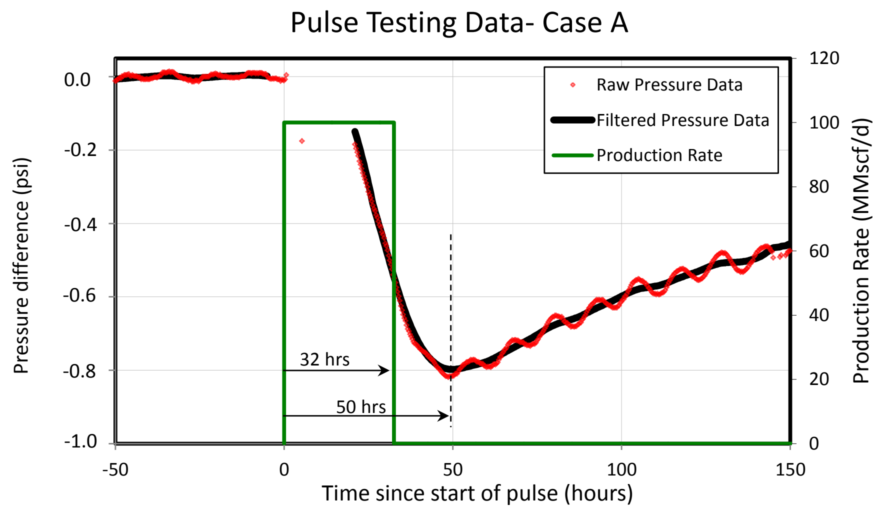

Figure 5 Pulse Testing Data for Case A

The tidal effects were filtered out to generate the black line (see Figure 5). In reality this was not necessary because minimum pressure, at about 50 hours, was also evident in the raw data. Nevertheless, the exact time was calculated by differentiating the filtered data and equating its value to zero. The necessary reservoir and fluid properties are summarised in the following table. The interconnected permeability is estimated to be ~600mD in accordance with Equation 7.

Table 3 Summary of parameters used for Case A

Parameter (unit)	Value
φ (fraction)	.30
μ (cP)	.026
c (psi^{-1})	1.5×10^{-4}
r (ft)	4000
t (hours)	50
t_l (hours)	18

It was also possible to calculate the pressure response, in accordance with Equation 6, by using the following parameter: height (h) of 100 ft and angle (α) of 360^o and an equivalent rate of 100MMSCFPD (or q=75,000 reservoir bbl/d). Figure 6 depicts data against the matched analytical model. Interestingly, the shape of the data pulse clearly exhibits radial coordinate characteristics.

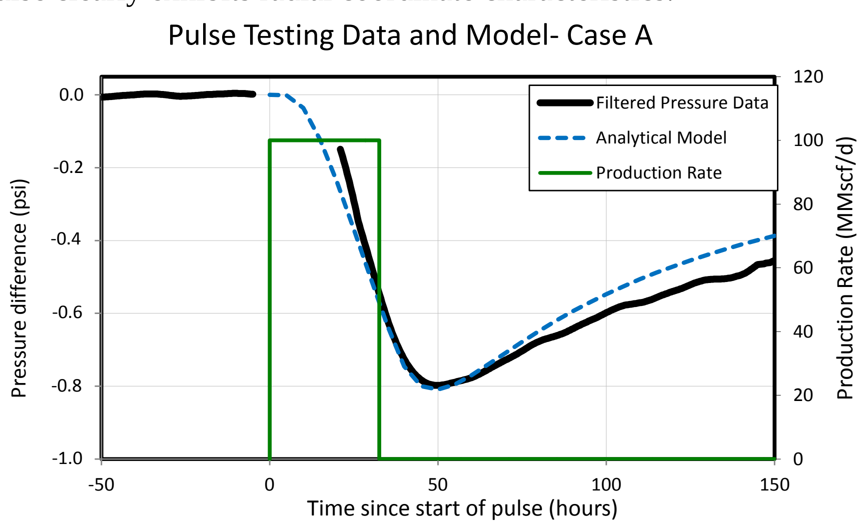

Figure 6 Pulse Testing Data and Model for Case A

The case study discussed above illustrates the value of simple pulse testing data. Providing the tests are designed appropriately and acquired data are of high quality, valuable subsurface information can be obtained from the reservoir in a relatively short time.

Case B

In this case, unlike the previous, the reservoir consists of multiple fluvial sand channels. The observation and producing wells were not completed in the same sand. Communication between these wells, however, was expected. Pulse testing proved valuable in confirming pressure communication between these, as shown in Figure 7 below. The producer generated a ~31-hour pulse at a maximum rate of 90,000 bbl/d (~120 MMscf/d).

In this case the tidal effects had to be filtered out, which was simply achieved by utilising a moving average of the tidal period. Raw and filtered pressure difference data are shown by red and black lines, respectively. The minimum pressure at the observation well was calculated to have occurred at $t \approx 54$ hrs with a value of t_l of 23 hours.

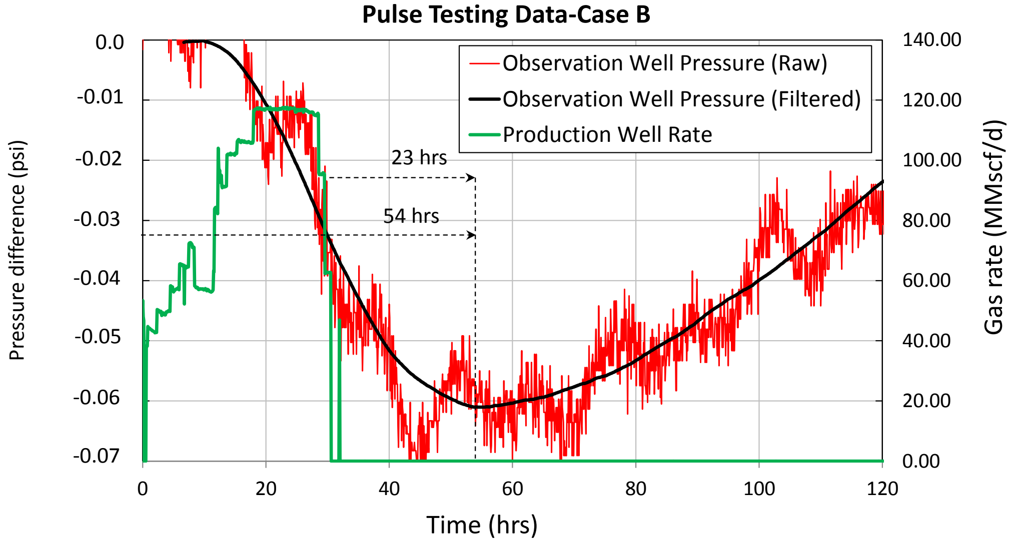

Figure 7 Pulse testing data for Case B

Given the following reservoir parameters the interconnected permeability was estimated to range from ~330 to ~650mD, dependent upon reservoir geometry. Further investigation of the shape of the pulse indicated that pressure in the area was increasing because of the effect of another well which had been shut in. Correcting for this effect indicated a channel flow regime, suggesting ~600md to be a more likely value of permeability.

Parameter (unit)	Value
φ (fraction)	.24
μ (cP)	.023
c (psi^{-1})	1.7×10^{-4}
x or r (ft)	3,500
t (hrs)	54
t_l (hrs)	23
Linear flow k (mD)	654
Radial flow k (mD)	327

Table 4 Summary of known data and calculated permeability values using pulse testing formulae

Emulating the pressure response by Equation 5 indicated that the observed pulse was attenuated by a factor of 40. A comparable response was simulated in a reservoir model by assuming communication (k_z/k_x=0.1) between sands in the proximity of the observation well.

Case C

In this case also, the producer and injector are completed in different sands, but separated by a greater distance. This made searching for the pulse more challenging. Figure 8 illustrates the production well rate and the observation well pressure. The plot depicts the pressure data within a range of 0.06 psi. The tidal noise is clearly visible, but pulse-related trends are not apparent. One may conclude, therefore, that these two wells are not in communication.

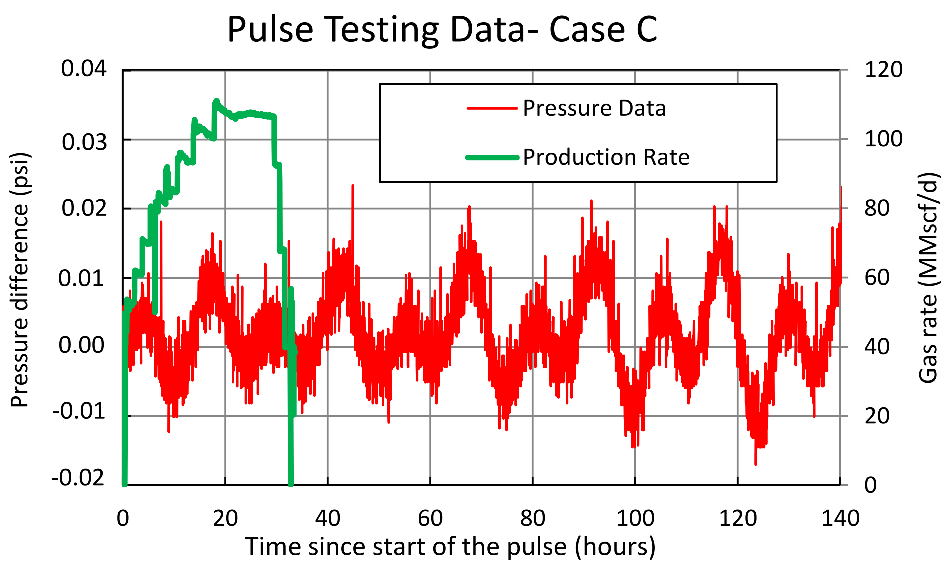

Figure 8 Pulse testing data for Case C showing a range of 0.08 psi

Further investigations, however, proved otherwise. By applying successive filters, it was possible to remove the high frequency noise components from the data. Figure 9 displays the filtered pressure data within a zoom range of 0.001 psi.

In the plot below, the timing of the minimum pressure occurs approximately ~90 hours after the start of a 32-hour pulse. Given these times, a distance of 8,000 ft and the above fluid properties, the interconnected permeability is estimated to be ~1,600mD for linear and ~800mD for radial flow regime.

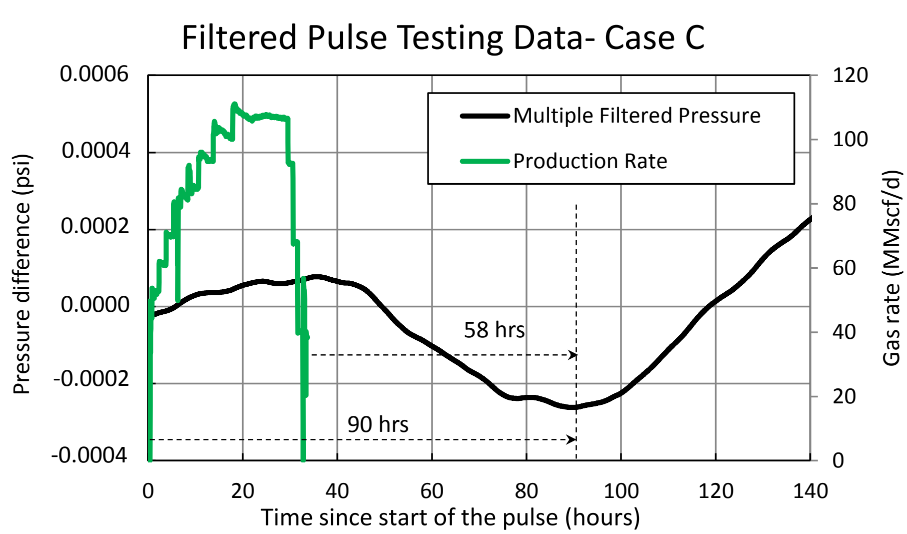

Figure 9 Filtered pulse testing data for Case C

From the shape of the pulse it appears that a radial regime (~800mD) is more likely. Efforts to model the interference with a reservoir simulator, by amplifying the impulse, were not successful. It was impossible to match both the amplitude and the time lag of the pulse. This is either because the geometry is too complex or because of the limitations of finite difference approximation, as described above. The latter is, however, suspected. It is also important to note, however, that pressure communication between the producer and injector clearly exists. Its quantification in the context of $\Delta P = f(q,t)$ will require more production than a short pulse test.

Conclusions

Pulse testing is a reliable and efficient method to determine communication between wells. Superposition was used to derive the pulse-test driven pressure disturbance as a function of time and distance in both linear and radial flow configurations. From these equations it was possible to derive very simple formulae to determine interconnected permeability for each of the above flow regimes. Because these are independent of flow rate or reservoir thickness, the resulting estimate of interconnected permeability is likely to be more definitive than a value derived from interference testing.

These analytical equations make it possible to interpret very subtle impulses which cannot be analysed by finite difference reservoir simulation alone, irrespective of how fine the grid is made. It is also possible to determine the effective reservoir thickness, or the geometry of the channel, if the wells are connected by the same reservoir exhibiting relatively homogeneous reservoir characteristics. For more complex cases, reservoir simulation can be used to generate a geometry, which matches the derived interconnected permeability and the amplitude of the pressure pulse.

References

Braisted, D. M., Spengier, R. M., Youle, R. A., Reservoir Description Through Pulse Testing in a Mature Field, SPE paper 22965, June 1993

Brigham, W.E., Planning and Analysis of Pulse Tests, JPT 618-624, May 1970

Ehlig-Economides, C. and Economides, M., Pressure Transient Analysis in an Elongated Linear Flow System, SPE Jounrnal, P 839-847, December 1985

El-Khatib, N., New Approach for Pulse Test Analysis, SPE paper 164597, April 2013

El-Khatib, N., Design and Analysis of Pulse Tests, Journal of Petroleum Science and Technogloy, 2011, p69-77

Johnson, C.R., Greenkorn, R.A., Woods, E.G., Pulse Tsing: A New Method for Describing Reservoir Flow Properties Between Wells, SPE paper 1517, Dec 1966

McKinley, M. R., Vela, S., Carlton, L.A., A Field Application of Pulse-Testing for Detailed Reservoir Description, SPE paper 1822, March 1968

Miller, F.G., Theory of Unsteady-State Influx of Water in Linear Reservoirs, Jounral of Inst. Pet., Nov 1962, 48, 467

Toth, B., and Megyery, M., Evaluation of Pulse Tests With Noise Suppressing, SPE Formation Evaluation Journal, P132-136, June 1997